that genetic analysis of single intestinal metaplastic glands may be helpful in detecting such genetic alterations.

Marked clinical and biological heterogeneity has been noted among human gastric cancers (1-3). However, possible genetic causes of genetic heterogeneity have not been fully investigated. In this study, we used tumor single-gland samples to look for heterogeneous populations within the same tumor. Our findings that 90% of tumors demonstrated heterogeneous composition within the same tumor, show that gastric cancers are genetically highly complex. On average, there were 4.2 genetic alterations per tumor. The high number of genetic alterations per tumor indicates that genetic instability may cause intratumoral heterogeneity, as seen in other human tumors (1,3,27,28), and be an underlying mechanism of gastric carcinogenesis. In addition, our findings suggest that a specific subclone cannot be selected in most gastric cancers during tumor progression. This is an important finding toward understanding the effectiveness of chemotherapy or radiotherapy in gastric cancers, because the existence of heterogeneous populations indicates no single target cell can be defined.

The degree of accumulated LOH (allelic imbalance) has been shown to be of prognostic value in various cancer types including gastric cancer, and a high degree of tumor LOH has been shown to be associated with tumor aggressiveness and a worse prognosis (29). In light of these findings, low and high rates of tumor LOH suggest low and high tumor behavioral aggressiveness, respectively. In some of the present cases, although minor-altered genotype (low LOH) was found in the pooled-gland sample, major-altered genotype (high LOH) was detected in the corresponding tumor single-gland sample. Our findings also indicate that 2 of 5 tumors showing a minor-altered genotype in the pooled-gland sample were classified as type II (composed of major-altered genotype) in the tumor single-gland sample. This finding suggests that highly aggressive subclones may exist within a tumor showing a low frequency of LOH in a pooled-gland sample (2/5, 40%). It is surprising that 40% of pooled-gland samples showing the minor-altered genotype contained a major-altered genotype in the corresponding tumor single-gland samples. On the other hand, in the present study, most of the carcinomas that were examined contained a minor-altered genotype of single tumor glands within the same tumor. One recent study has shown that high-LOH tumors may have a higher rate of response to chemotherapy (29,30). However, in general, the majority of patients with gastrointestinal cancers are thought to obtain a poor response to chemotherapy without survival benefit (29,30). Although the genetic reason for the discrepancy remains unknown, an explanation may be that the minor-altered genotype gland is a supply source to the major-altered genotype gland. Therefore, a minor-altered genotype gland may co-exist with a major-altered genotype gland within the same tumor (3).

In the present study, genotypic pattern for a single-gland sample was classified into 5 groups. Although types I and II were the most frequent genotypic patterns (17/20, 85%), type IV, a tumor genotype showing predominantly minor-altered glands, was relatively rare (3/20, 15%). These findings suggest that single tumor glands with multiple genetic alterations may cause subclonal expansions in different areas within the same tumor, leading to occupation of the whole tumor mass in gastric cancers.

The general strategy of identification of individuals at high risk for progression to cancer offers promising possibilities for cancer prevention, and this approach largely depends on early detection. Therefore, it is important to evaluate GIM, which is generally thought to be a precancerous condition in gastric cancer (12,18). Furthermore, a previous study has shown that GIM is closely associated with *Helicobacter pylori* infection (31). However, little is known about the genetic events responsible for initiation and progression of gastric cancer (32,33). According to an investigation by Ochiai *et al*, although *p53* mutations known to play a key role in human neoplastic progression were identified in GIM, they were detected in only 10 of 756 (1.3%) histological sections (18). This finding indicates that it is difficult to identify such subtle genetic alterations in intestinal metaplastic glands. Genetic analysis of a single gland may enable us to identify subtle genetic alterations in GIM. Therefore, we used isolated single glands in the current study to address the issue of whether molecular alterations occur in GIM. In this study, although no genetic alterations were detected in pooled samples of intestinal metaplastic glands, alterations were frequently found in the corresponding single intestinal metaplastic gland samples. This suggests that intestinal metaplastic glands have a markedly heterogeneous composition. This study is the first to identify that expansive microsatellite alterations are seen in samples of intestinal metaplastic glands. These data indicate that irreversible genetic changes have already occurred in morphologically non-neoplastic gastric mucosa with intestinal metaplasia, and they support the hypothesis that GIM may be a precursor lesion of gastric cancer.

The present study has demonstrated that multiple genetic alterations are frequently found in nonmetaplastic glands. This is a surprising finding and the first study to identify genetic alterations in histologically normal gastric glands. This finding suggests that accumulation of genetic alterations occurs not only in metaplastic glands but also in nonmetaplastic glands, and that genetic alterations in gastric epithelial cells during chronic gastritis may contribute to an increased risk of gastric cancer (34).

In conclusion, single tumor glands can be useful for investigating genetic alterations in gastric cancers and gastric intestinal metaplasia. The present data indicate that most carcinomas and GIM are genetically heterogeneous. Recently, public policy strategies have been suggested for identification of patients at risk for *H. pylori*-related gastric malignancy (35,36). The thrust of this policy is that eradication of *H. pylori* infection earlier rather than later in life is anticipated to be more beneficial, because gastric intestinal metaplasia is expected to occur later in life. Our finding that multiple genetic alterations are found in single intestinal metaplastic glands may support this opinion.

Acknowledgements

We gratefully acknowledge the technical assistance of Miss E. Sugawara and Mr. T. Kasai. We also thank members of the Division of Pathology, Central Clinical Laboratory, Iwate Medical University, for their support.

References

1. Nowel PC: The clonal evolution of tumor cell populations. Science 194: 23-28, 1976.
2. Ishii M, Sugai T, Habano W and Nakamura S: Analysis of Ki-ras gene mutations within the same tumor using a single tumor crypt in colorectal carcinomas. J Gastroenterol 39: 544-549, 2004.
3. Sugai T, Habano W, Jiao Y-F, *et al*: Analysis of allelic imbalances at multiple cancer-related chromosomal loci and microsatellite instability within the same tumor using a single tumor gland from colorectal carcinomas. Int J Cancer 114: 337-345, 2005.
4. Fearon ER and Vogelstein B: A genetic model for colorectal tumorigenesis. Cell 61: 759-767, 1990.
5. Chung YJ, Kim KM, Choi JR, Choi SW and Rhyu MG: Relationship between intratumor histological heterogeneity and genetic abnormalities in gastric carcinoma with microsatellite instability. Int J Cancer 82: 782-788, 1999.
6. Iwamatsu H, Nishikura K, Watanabe H, *et al*: Heterogeneity of p53 mutational status in the superficial spreading type of early gastric carcinoma. Gastric Cancer 4: 20-26, 2001.
7. Sugai T, Uesugi N, Habano W, *et al*: DNA mapping of gastric cancers using flow cytometric analysis. Cytometry 42: 270-276, 2000.
8. Nakayama S, Nakayama K, Takebayashi Y, *et al*: Allelotypes as potential prognostic markers in ovarian carcinoma treated with cisplatin-based chemotherapy. Int J Mol Med 11: 621-625, 2003.
9. Barratt PL, Seymour MT, Stenning SP, *et al*: UKCCCR AXIS trial collaborators. Adjuvant X-ray and Fluorouracil Infusion Study. UKCCCR AXIS trial collaborators. DNA markers predicting benefit from adjuvant fluorouracil in patients with colon cancer: a molecular study. Lancet 360: 1381-1391, 2002.
10. Day DW, Jass JR, Price AB, Shepherd NA, Sloan JM, Talbot IC, Warren BF and Williams GT (eds): Morson and Dawson's Gastrointestinal Pathology. 4th edition, Blackwell Science, 114-115, 2003.
11. Mutoh H, Sakurai S, Satoh K, *et al*: Development of gastric carcinoma from intestinal metaplasia in Cdx2-transgenic mice. Cancer Res 64: 7740-7747, 2004.
12. Morgan C, Jenkins GJ, Ashton T, *et al*: Detection of p53 mutations in precancerous gastric tissue. Br J Cancer 89: 1314-1319, 2003.
13. Tatematsu M, Tsukamoto T and Mizoshita T: Role of *Helicobacter pylori* in gastric carcinogenesis: The origin of gastric cancers and heterotopic proliferative glands in Mongolian Gerbils. Helicobacter 10: 97-106, 20056.
14. Baracchini P, Fulcheri E and Lapertosa G: Patterns of intestinal metaplasia in gastric biopsies. A comparison of different histochemical classifications. Histochem J 23: 1-9, 1991.
15. Matsukura N, Suzuki K, Kawachi T, *et al*: Distribution of marker enzymes and mucin in intestinal metaplasia in human stomach and relation to complete and incomplete types of intestinal metaplasia to minute gastric carcinomas. J Natl Cancer Inst 65: 231-240, 1980.
16. Mirza ZK, Das KK, Slate J, *et al*: Gastric intestinal metaplasia as detected by a monoclonal antibody is highly associated with gastric adenocarcinoma. Gut 52: 807-812, 2003.
17. Blok P, Craanen ME, Offerhaus GJ and Tytgat GN: Gastric carcinoma: clinical, pathogenic, and molecular aspects. QJM 90: 735-749, 1997.
18. Ochiai A, Yamauchi Y and Hirohashi S: p53 mutations in the non-neoplastic mucosa of the human stomach showing intestinal metaplasia. Int J Cancer 69: 28-33, 1996.
19. Sugai T, Habano W, Nakamura S, *et al*: Genetic alterations in DNA diploid, aneuploid and multiploid colorectal carcinomas identified by the crypt isolation technique. Int J Cancer 88: 614-619, 2000.
20. Arai T and Kino I: Morphometrical and cell kinetic studies of normal human colorectal mucosa: Comparison between the proximal and the distal large intestine. Acta Pathol Jpn 39: 725-730, 1989.
21. Japanese Research Society for Gastric Cancer: The General Rules for the Gastric Cancer Study. 12th edition, Kanehara-Shuppan, Tokyo, pp64-89, 1993.
22. Nakamura S, Goto J, Kitayama M and Kino I: Application of the crypt-isolation technique to flow-cytometric analysis of DNA content in colorectal neoplasms. Gastroenterology 106: 100-107, 1994.
23. Sugai T, Habano W, Uesugi N, *et al*: Three independent genetic profiles based on mucin expression in early differentiated-type gastric cancers - a new concept of genetic carcinogenesis of early differentiated-type adenocarcinomas. Mod Pathol 17: 1223-1234, 2004.
24. Jiao Y-F, Sugai T, Habano W, Suzuki M, Takagane A and Nakamura S: Analysis of microsatellite alterations in gastric carcinoma by applying the crypt isolation technique. J Pathol 204: 200-207, 2004.
25. Habano W, Sugai T, Nakamura S and Yoshida T: A novel method for gene analysis of colorectal carcinomas using a crypt isolation technique. Lab Invest 74: 933-940, 1996.
26. Sugai T, Takahashi H, Habano W, *et al*: Analysis of genetic alterations, classified according to their DNA ploidy pattern, in the progression of colorectal adenomas and early colorectal carcinomas. J Pathol 200: 168-176, 2003.
27. Faquin WC, Fitzgerald JT, Boynton KA and Mutter GL: Intratumoral genetic heterogeneity and progression of endometrioid type endometrial adenocarcinomas. Gynecol Oncol 78: 152-157, 2000.
28. Matsumoto T, Fujii H, Arakawa A, *et al*: Loss of heterozygosity analysis shows monoclonal evolution with frequent genetic progression and divergence in esophageal carcinosarcoma. Hum Pathol 35: 322-327, 2004.
29. Grundei T, Mueller J, Scholz M, *et al*: Loss of heterozygosity and microsatellite instability as predictive markers for neoadjuvant treatment in gastric carcinoma. Clin Cancer Res 6: 4782-4788, 2000.
30. Ott K, Vogelsang H, Ott K, *et al*: Chromosomal instability rather than p53 mutation is associated with response to neoadjuvant cisplatin-based chemotherapy in gastric carcinoma. Clin Cancer Res 9: 2307-2315, 2003.
31. Hirayama F, Takagi S, Yokoyama Y, Yamamoto K, Iwao E and Haga K: Long-term effects of *Helicobacter pylori* eradication in Mongolian gerbils. J Gastroenterol 37: 779-784, 2002.
32. Boussioutas A, Li H, Liu J, *et al*: Distinctive patterns of gene expression in premalignant gastric mucosa and gastric cancer. Cancer Res 63: 2569-2577, 2003.
33. Sugai T, Habano W, Nakamura S, *et al*: Correlation of histological morphology and tumor stage with molecular genetic analysis using microdissection in gastric carcinomas. Diagn Mol Pathol 7: 235-240, 1998.
34. Yao Y, Tao H, Park DI, Sepulveda JL and Sepulveda AR: Demonstration and characterization of mutations induced by *Helicobacter pylori* organisms in gastric epithelial cells. Helicobacter 11: 272-286, 2006.
35. Hunt RH: Will eradication of *Helicobacter pylori* infection influence the risk of gastric cancer? Am J Med 117 (Suppl 5A): S86-S91, 2004.
36. Yoo EJ, Park SY, Cho NY, Kim N, Lee HS and Kang GH: *Helicobacter pylori*-infection-associated CpG island hypermethylation in the stomach and its possible association with polycomb repressive marks. Virchows Arch 452: 515-524, 2008.

GASTROENTEROLOGY 2009;137:902–913

BASIC—ALIMENTARY TRACT

Elevated Dnmt3a Activity Promotes Polyposis in *Apc*^{Min} Mice by Relaxing Extracellular Restraints on Wnt Signaling

MICHAEL S. SAMUEL,* HIROMU SUZUKI,‡ MICHAEL BUCHERT,* TRACY L. PUTOCZKI,* NIALL C. TEBBUTT,* THERÉSE LUNDGREN-MAY,* ALIKI CHRISTOU,* MELISSA INGLESE,* MINORU TOYOTA,§ JOAN K. HEATH,* ROBYN L. WARD,‖ PAUL M. WARING,* and MATTHIAS ERNST*

*Ludwig Institute for Cancer Research, Royal Melbourne Hospital, Victoria, Australia; ‡First Department of Internal Medicine, Sapporo Medical University, Sapporo, Japan; §Department of Molecular Biology, Cancer Research Institute, Sapporo Medical University, Sapporo, Japan; ‖Prince of Wales Clinical School and UNSW Cancer Centre, University of New South Wales, Sydney, Australia

BACKGROUND & AIMS: Aberrant DNA methylation is a common early event in neoplasia, but it is unclear how this relates to dysregulation of DNA (cytosine-5) methyltransferases (Dnmts). Here we use knock-in transgenic mice to investigate the consequences of intestinal epithelium-specific overexpression of de novo Dnmt3a. **METHODS:** A novel gene targeting strategy, based on the intestinal epithelium-specific, uniform expression of the A33 glycoprotein, is employed to restrict Dnmt3a overexpression in homozygous *A33*^{Dnmt3a} mutant mice. **RESULTS:** *A33*^{Dnmt3a} mice infrequently develop spontaneous intestinal polyps. However, when genetically challenged, tumor multiplicity in *A33*^{Dnmt3a};*Apc*^{Min} compound mice is 3-fold higher than in *Apc*^{Min} mice. Although we observe a requirement for spontaneous loss of heterozygosity of the adenomatous polyposis coli (*Apc*) gene to trigger tumorigenesis in *Apc*^{Min} mice, lesions in *A33*^{Dnmt3a};*Apc*^{Min} mice frequently retain the wild-type *Apc* allele. However, epithelia from normal mucosa and polyps of *A33*^{Dnmt3a};*Apc*^{Min} mice show hypermethylation-mediated transcriptional silencing of the Wnt antagonists *Sfrp5*, and to a lesser extent, *Sfrp1* and increased nuclear β-catenin alongside activation of the Wnt-target gene *Axin2/Conductin*. Conversely, enforced Sfrp5 expression suppresses canonical Wnt-signaling more effectively in wild-type than in *Apc*^{Min} cells. **CONCLUSIONS: Aberrant activation of the canonical Wnt pathway, either by mono-allelic *Apc* loss or transcriptional silencing of *Sfrp5* is largely insufficient to promote polyposis, but epistatic interactions between these genetic and epigenetic events enables initiation and promotion of disease. This mechanism is likely to play a role in human colorectal cancer, because we also show that elevated *DNMT3A* expression coincides with repressed *SFRP5* and enhanced *AXIN2/CONDUCTIN* expression in paired patient biopsies.**

Epigenetic modifications including DNA (cytosine-5) methylation are critical for the interpretation of genetic information and ensure appropriate, cell type-specific gene expression. Consequently, the presence of altered DNA methylation[1] and dysregulation of DNA-methyltransferases (Dnmt)[2,3] correlates with a number of pathologic conditions, including cancer. A global decrease in cytosine methylation, usually within repetitive sequences and intergenic regions, is a hallmark of human cancer,[4] and promotes genetic instability and tumors in mice. Similarly, age-related, genome-wide hypomethylation of centromeric regions in humans[5] correlates with chromosomal abnormalities, predisposes to genetic damage, and increases the risk of tumor development. Concomitantly, cancer cell genome-associated regions of cytosine hypermethylation[6] within CpG islands of promoter regions results in transcriptional silencing of genes with tumor suppressor activity. Because aberrant DNA methylation patterns are maintained throughout subsequent rounds of cell division, they have been proposed to contribute to carcinogenesis.[7]

Methylation of mammalian DNA is carried out by multimeric protein complexes comprising members of the Dnmt protein family. Whereas Dnmt1 requires hemi-methylated DNA as a template to faithfully maintain established methylation marks, the Dnmt3 de novo methyltransferases act on unmethylated cytosine residues in double-stranded DNA. Simultaneous inactivation of *Dnmt3a* and *Dnmt3b* results in embryonic lethality of mice, owing to the requirement of these enzymes for genetic imprinting and X chromosome inactivation during embryogenesis. Although the individual ablation of de novo Dnmts is compatible with life, it alters intestinal tumorigenesis

Abbreviations used in this paper: APC, adenomatous polyposis coli; CRC, colorectal cancer; DKK, Dickkopf; Dnmt, DNA-methyltransferases; GSK-3β, glycogen synthase kinase-3b; IEC, intestinal epithelial cells; LOH, loss of heterozygosity; LSL, lox(P)-flanked transcription terminator; MEFs, mouse embryo fibroblasts; MSP, methylation-specific PCR; qPCR, quantitative reverse transcriptase polymerase chain reaction; SFRP, secreted frizzled-related proteins; TCF, T-cell transcription factor; WIF-1, Wnt inhibitor factor-1.

0016-5085/09/$36.00
doi:10.1053/j.gastro.2009.05.042

when challenged in the polyposis-prone Apc^{Min} background.[8] Meanwhile, overexpression of Dnmt in mammalian cells results in aberrant DNA methylation and promotes cellular transformation,[9] which may explain the failure to generate global Dnmt gain-of-function mice.

Despite the frequent association between epigenetic DNA modification and cancer, it remains unclear whether tumor-associated regional hypermethylation is a cause or a consequence of disease. Hypermethylation is often detected in early dysplastic lesions, and some tumor characteristics correlate with epigenetic silencing of tumor-relevant genes.[10] However, unbiased screens designed to identify hypermethylated regions in tumor-derived DNA yielded many potential bystander genes not directly involved in pathogenesis.[11] Similarly, loss-of-function studies on maintenance DNA methylation could not establish unequivocally whether cancer-specific hypermethylation occurred regionally or globally. Interestingly, up-regulation of the de novo DNA methyltransferases DNMT3A and DNMT3B has been reported as a feature of the colorectal adenoma–carcinoma sequence.[12] Tissue-specific (over-)expression of Dnmts in vivo is therefore required to clarify whether de novo gene methylation is a driver of tumor development, rather than an adaptive change associated with tumorigenesis,[13] and whether increased expression of de novo DNMTs is capable of directly driving de novo gene methylation.

The development of colorectal cancer (CRC) involves cumulative alterations in distinct tumor-suppressors and proto-oncogenes.[14] In human sporadic CRC, these mutations affect the *Adenomatous Polyposis Coli* (*APC*), and less frequently, *CTNNB1/β-catenin* or *AXIN2/CONDUCTIN* genes,[15] which all encode components of the canonical Wnt signaling pathway. Inherited *APC* loss-of-function mutations occur in familial adenomatous polyposis kindreds, because APC acts as a gatekeeper for entry of intestinal epithelial cells (IEC) into the adenoma-to-carcinoma progression.[16] In wild-type cells, receptor-binding of secreted WNT-family proteins triggers cytosolic stabilization and accumulation of β-catenin, which forms a complex with T-cell transcription factor (TCF) to induce target gene expression. Along with APC, negative regulators of this signaling cascade include other components of the cytosolic β-catenin destruction complex such as glycogen synthase kinase-3b (GSK-3β) and AXIN2/CONDUCTIN. Meanwhile, the activity of WNT ligands is antagonized by extracellular proteins, such as the Dickkopf (DKK) and secreted frizzled-related proteins (SFRP), as well as Wnt inhibitor factor-1 (WIF-1).[17]

Here, we show that restricting Dnmt3a transgene expression to IECs in $A33^{Dnmt3a}$ knock-in mutant mice is sufficient to elicit infrequent tumors. However, when genetically challenged on an Apc^{Min} background, intestinal polyposis in corresponding $A33^{Dnmt3a}$;Apc^{Min} mice is significantly augmented. We attribute this increase to a cooperative effect between mutations in 2 negative Wnt-pathway regulators, namely germ-line inactivation of 1 *Apc* allele and Dnmt3a-mediated epigenetic silencing of the *Sfrp5* gene.

Materials and Methods

Mice and Human Samples

Mice homozygous for the $A33^{Dnmt3a}$ knock-in mutations were generated by standard procedures (see Supplementary Methods) and propagated on a C57B/B6 background. Health of experimental mice was monitored according to guidelines approved by the Ludwig Institute's Animal Ethics Committee.

Nine CRC and paired normal colonic mucosa were randomly selected from a prospectively collected series of individuals who had undergone curative resection. Written informed consent was obtained from all individuals, and the study was approved by the St. Vincent's Campus Human Research Ethics Committee. The clinical, pathologic, and molecular characteristics of these patient samples have been documented.[18]

mRNA Expression Analysis, Cell Culture and Transfections, Methylation Analysis, Histology, Immunocytochemistry, and Immunohistochemistry

Quantitative reverse transcriptase polymerase chain reaction (qPCR) expression analysis was carried out using SYBR-Green dye and data were expressed relative to expression of glyceraldehyde-3-phosphate dehydrogenase (GAPDH) or 18s RNA. Luciferase reporter activity in mouse embryo fibroblasts (MEFs) stimulated with Wnt3a-conditioned medium was determined using dual-Luciferase technology. Bisulfite treatment of genomic DNA and methylation-specific PCR (MSP) was carried out as described.[19] Formalin-fixed specimens were prepared and stained following standard histology procedures (for more details see Supplementary Methods).

Apc Loss of Heterozygosity Determination

Parts of exon 16 containing the *Min* allele specific T>A substitution were PCR-amplified (Supplementary Table 1) and the gel-purified amplicons sequenced on an ABIprism 377 DNA sequencer (Applied Biosystems, Foster City, CA).

Statistical Analysis

Polyp numbers from $A33^{Dnmt3a}$;Apc^{Min} and $A33^{wt}$;Apc^{Min} mice were analyzed using the unpaired *t*-test to determine statistical significance.

Results

Novel Gene Targeting Strategy to Restrict Transgene Expression to the Intestinal Epithelium

To determine whether regional hypermethylation is sufficient to initiate tissue-specific tumorigenesis, we

restricted overexpression of Dnmt3a to murine intestinal epithelium using a novel knock-in gene targeting strategy. We chose the *gpA33* gene locus because it confers uniform expression of the transmembrane A33 antigen glycoprotein to all IEC along the entire intestinal tract from the gastric pylorus to the rectum.[20] To retain activity of endogenous *gpA33* and to faithfully confer its temporal and spatial expression pattern to the transgene, we targeted a cDNA encoding Dnmt3a to the 3′-untranslated region immediately downstream of the A33 coding sequence, preceded by a lox(P)-flanked transcription terminator (LSL) cassette (Figure 1*A*; Supplementary Figure 1*A*). Breeding of the corresponding $A33^{\text{LSL-Dnmt3a}}$ mice with E2a:Cre transgenic "deletor" mice[21] excised the LSL cassette in the germline and resulted in transgene expression (Supplementary Figure 1*B*) and an associated 4-fold increase of enzymatic methyltransferase activity in IECs from $A33^{\text{Dnmt3a}}$ mice (Figure 1*B*). We used qPCR and Northern analysis on isolated epithelia to establish that transgene expression in $A33^{\text{Dnmt3a}}$ mice resulted in increased abundance of total *Dnmt3a* transcripts, while the abundance of endogenous *Dnmt3b* transcripts remained unchanged (Figure 1C; Supplementary Figure 1C). Reproducible and uniform overexpression of Dnmt3a protein within all IECs along the rostrocaudal axis of the small intestine and colon of $A33^{\text{Dnmt3a}}$ mice was also confirmed by immunohistochemistry (Figure 1*D*). Furthermore, transgene expression from the *A33-Dnmt3a* bicistronic RNA did not interfere with the uniform distribution pattern of the A33 glycoprotein.

Although homozygous $A33^{\text{Dnmt3a}}$ ($n = 140$), $A33^{\text{LSL-Dnmt3a}}$ ($n = 120$), and $A33^{\text{wt}}$ ($n = 78$) mice were histopathologically indistinguishable (Supplementary Figure 2), 6 $A33^{\text{Dnmt3a}}$ mice ≥18 months old developed either macroscopic adenomatous polyps in the proximal or middle portion of the small intestine (1 mouse each), the cecum (1 mouse), the colon (1 mouse), or displayed intestinal bleeding in the absence of macroscopic lesions (2 mice). The tumors exhibited tubulovillous architecture reminiscent of polyps arising in Apc^{Min} mice (Figure 2*A*), whereas the widespread transgene expression throughout the tumor epithelium (Figure 2*B*) was consistent with retention of A33 antigen expression in CRC lesions.[22] Because aberrant promoter hypermethylation and associated silencing of *APC* and *SFRP* occurs in CRC cell lines,[23,24] we used an antibody directed against the very carboxyl-terminal domain of Apc[25] to assess for possible reduction of full-length Apc protein within the neoplastic lesions as well as MSP analysis and bisulfite conversion sequencing to determine promoter methylation status of Apc and Sfrps. We observed neither down-regulation of Apc protein (Figure 2C) nor *Apc* promoter hypermethylation as determined by MSP analysis and bisulfite conversion sequencing (Figure 2*E*, *F*). However, the corresponding analysis revealed specific methylation of *Sfrp1* and *Sfrp5*, but not of *Sfrp2* (Figure 2*E*, *F*). Furthermore, qPCR analysis (Figure 2*D*) revealed elevated expression of the bona fide Wnt target genes *CD44*, *Myc*, and *Axin2/Conductin*[26] in colonic tumors from $A33^{\text{Dnmt3a}}$ mice at levels comparable to those observed in the subset of $A33^{\text{Dnmt3a}}$;Apc^{Min} mouse tumors, where Wnt target gene activation occurs as a consequence of loss of heterozygosity (LOH) of the wild-type *Apc* allele (see below). Restricting overexpression of *Dnmt3a* to the intestinal epithelium therefore, does not affect its development, architecture, or homeostasis, but predisposes to intestinal tumorigenesis. However, the long latency period in the proportion of affected $A33^{\text{Dnmt3a}}$ mice suggests a requirement for additional (epi-)genetic events[27] and/or clonal selection of individual cells with silenced *Sfrp1* and *Sfrp5* loci for the development of disease.

Elevated Intestinal Polyposis in $A33^{Dnmt3a}$;Apc^{Min} Mice

To determine whether *Dnmt3a*-associated regional DNA hypermethylation cooperates with a phenotypically "dormant" germ-line mutation, we assessed intestinal polyposis in Apc^{Min} and $A33^{\text{Dnmt3a}}$;Apc^{Min} mice that were established as colonies on a mixed 129/Sv × C57Bl/6 genetic background. Compared with Apc^{Min} mice, their $A33^{\text{Dnmt3a}}$;Apc^{Min} counterparts showed a 3-fold higher number of macroscopic (>1 mm) polyps within the distal small intestine and colon on either genetic background, with a similar trend extended to the middle, but not the proximal small intestine (Figure 3*A*). These observations were also confirmed in cohorts of the corresponding mice established on an inbred C57Bl/6 backgrounds (data not shown) to control for effects of modifier loci including the epigenetically regulated *Mom1*[28] locus. Similar to our observation in single mutant $A33^{\text{Dnmt3a}}$ mice (Figure 3*A*), tumors in $A33^{\text{Dnmt3a}}$;Apc^{Min} mice also retained uniform and persistent transgene expression in IECs without affecting the expression of endogenous Dnmt3b (Supplementary Figure 3*A*). Furthermore, the colons of $A33^{\text{Dnmt3a}}$;Apc^{Min} mice contained larger, clustered tumors when compared with Apc^{Min} colons (Figure 3*B*; Supplementary Figure 3*B*). Because methylation of the *H19/DMR* imprinting control region was unaffected in $A33^{\text{Dnmt3a}}$;Apc^{Min} mice (Supplementary Figure 4) the augmented tumor size in these mice appears to be unrelated to the previously proposed mechanism by which increased polyp growth in $Col1A1^{\text{Dnmt3b}}$;Apc^{Min} mice correlated with *H19/DMR* methylation and the associated restoration of biallelic *Igf2* expression.[29]

Wnt-Signaling Is Aberrantly Activated Without Apc LOH in $A33^{Dnmt3a}$;Apc^{Min} Mice

Epithelia of all polyps from $A33^{\text{Dnmt3a}}$;Apc^{Min} mice ($n = 21$) and Apc^{Min} mice ($n = 12$), but not of adjacent unaffected mucosa, exhibited nuclear accumulation of β-catenin (Figure 4*A*), indicative of aberrant canonical Wnt signaling. Whereas polyps from Apc^{Min} mice had all

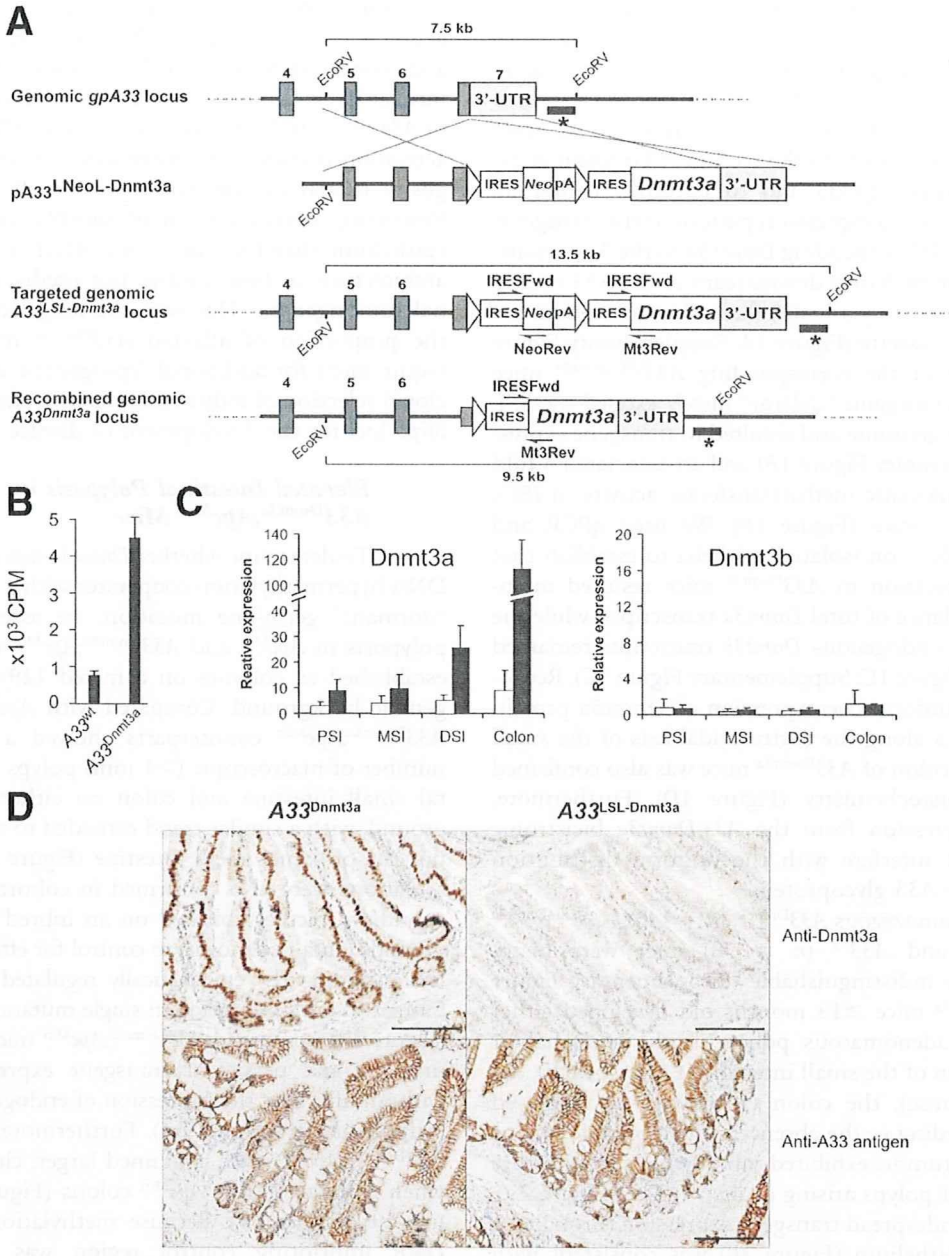

Figure 1. Enforced Dnmt3a transgene expression in $A33^{Dnmt3a}$ "knock-in" mutant mice. (*A*) Schematic depiction of the targeting strategy devised to generate mutant *gpA33* alleles. The targeting vector $pA33^{LNeoL\text{-}Dnmt3a}$ contains a lox(P) site-flanked (▷), promoterless IRES-neomycin phosphotransferase (*Neo*) and a promoterless IRES-*Dnmt3a* expression cassette and its homologous recombination in ES cells yields the $A33^{LSL\text{-}Dnmt3a}$ allele. Upon Cre-mediated recombination, the lox(P)-flanked IRES-*Neo*-pA cassette is excised and yields the $A33^{Dnmt3a}$ allele. A diagnostic *Eco*RV digest together with a radiolabeled DNA probe (*) was used to identify the different *gpA33* alleles with the corresponding fragment sizes indicated. Locations of the genotyping PCR primers are indicated by half-arrows and the numbered exons, polyadenylation site (pA) and 3′-untranslated region (3≥-UTR) of the *gpA33* gene are shown by boxes. (*B*) DNA methyltransferase activity in IECs derived from $A33^{wt}$ and $A33^{Dnmt3a}$ mice as determined by transfer of [^{14}C]-labeled methyl groups to the acceptor substrate poly-dI.dC. Mean ± SD, $n = 3$. (*C*). qPCR analysis for *Dnmt3a* and *Dnmt3b* expression in intestinal epithelium prepared from the proximal (PSI), middle (MSI), and distal small intestines (DSI) as well as the colons of 3-month-old wild-type (*open bars*) or $A33^{Dnmt3a}$ mice (*filled bars*). Data were normalized against expression of the house-keeping gene *Gapdh*. Mean ± SD; $n = 3$. (*D*) Imunohistochemical analysis of Dnmt3a (*upper panels*) and A33 (*lower panels*) on small intestines from $A33^{LSL\text{-}Dnmt3a}$ and $A33^{Dnmt3a}$ mice. Scale bar represents 50 μm.

uniformly lost expression of full-length Apc protein, its expression was retained in approximately one third of polyps collected from $A33^{Dnmt3a}$;Apc^{Min} mice (Figure 4*A*; Supplementary Figure 5*A*). We confirmed these observations genetically by amplifying the Apc^{Min} allele-specific TTG (Leu_{580}) to TAG (Stop) transversion in exon 16 in DNA isolated from tumors of the 2 genotypes. All lesions ($n = 25$) analyzed from Apc^{Min} mice revealed a <25%

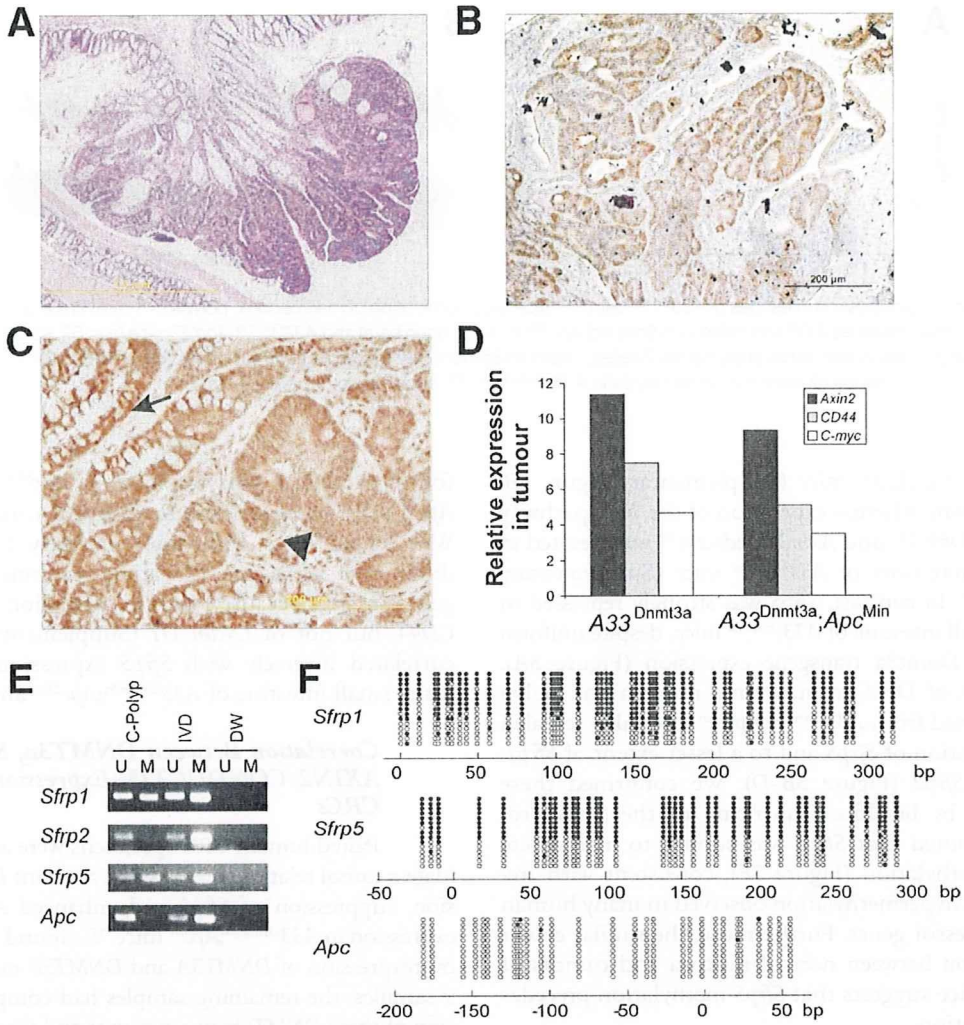

Figure 2. Spontaneous tumor formation in $A33^{Dnmt3a}$ mice coincides with *Sfrp* hypermethylation. (*A*) Hematoxylin and eosin-stained section through a colonic polyp from a 20-month-old $A33^{Dnmt3a}$ mouse. Scale bar represents 1 mm. (*B*). Dnmt3a-specific immunohistochemical staining of a colonic polyp from a $A33^{Dnmt3a}$ mouse. Scale bar represents 200 μm. (*C*) Apc-specific immunohistochemical staining of colonic sections from a 15-month-old $A33^{Dnmt3a}$ mouse shows similar intensity of full-length protein staining between dysplastic (*arrow head*) and surrounding normal epithelium (*arrow*). Scale bar represents 200 μm. (*D*) qPCR analysis of expression of the canonical Wnt-signaling target genes *Axin2/Conductin, CD44* and *c-myc* in a colonic polyp from $A33^{Dnmt3a}$ $A33^{Dnmt3a}$;Apc^{Min} mice. Data were normalized against expression of the house keeping gene *Gapdh*. (*E*) MSP analysis of genomic DNA derived from a colonic tumor arising in a 20-month-old $A33^{Dnmt3a}$ mouse. M, methylated; U, unmethylated; IVD, in vitro methylated DNA. (*F*) Bisulfite sequencing analysis of DNA from the tumor described in (*A*) with each vertical line referring to a CpG dinucleotide at the indicated position relative to the transcriptional start site. After bisulfite treatment, DNA was subcloned and sequenced. Horizontal lines represent individual sequences with open and full circles denoting unmethylated and methylated CpG residues, respectively.

contribution of the Apc^{wt} specific TTG haplotype (Figure 4*B*), consistent with LOH and the residual Apc^{wt} haplotype being contributed by either mesenchymal components within the polyp or contaminating adjacent normal mucosa. However, 9 of 28 polyps from $A33^{Dnmt3a}$;Apc^{Min} mice showed similar contribution from the 2 haplotypes (Figure 4*B*), suggesting maintenance of *Apc* heterozygosity in >30% of polyps, which coincided with the lack of *Apc* hypermethylation (Figure 4*C*; Supplementary Figure 5*B*). Collectively, our results suggest that roughly 1 in 3 macroscopic tumors in $A33^{Dnmt3a}$;Apc^{Min} mice showed activated (nuclear) β-catenin in the presence of 1 remaining, transcriptionally active wild-type *Apc* allele.

Sfrp5 Is Epigenetically Silenced in Apc^{Min};$A33^{Dnmt3a}$ Mice

Since expression of the DNA mismatch repair enzyme encoding *Mlh1* gene, which is often silenced in CRCs,[30] was not repressed in $A33^{Dnmt3a}$ mice (Supplementary Figure 6*A*), we hypothesized that *Dnmt3a*-mediated epigenetic changes may instead suppress genes that limit canonical Wnt signaling. However, expression of *Gsk-3*β and *Wif-1* remained comparable between normal mucosa

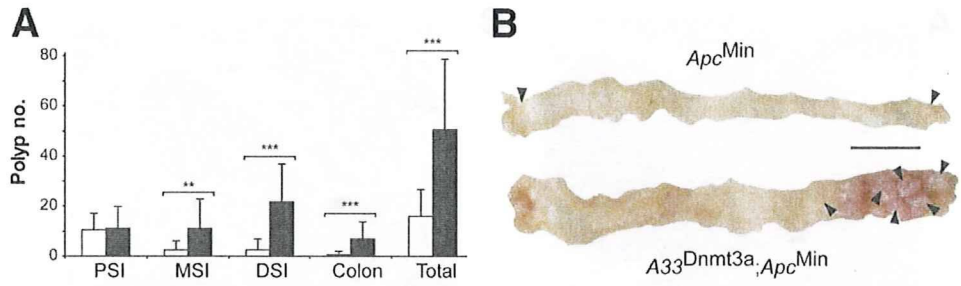

Figure 3. Enhanced polyposis in intestines of $A33^{Dnmt3a}$;Apc^{Min} mice. (*A*) Enumeration of macroscopic polyps (>1 mm) in the proximal (PSI), middle (MSI), and distal small intestines (DSI) and colon of 6-9mo old Apc^{Min} (n = 32; open bars) and $A33^{Dnmt3a}$;Apc^{Min} mice (n = 57; solid bars). Significance was assigned using P-values derived by applying the 2-tailed, unpaired Student t-test. (*B*) Longitudinally opened colons from 3-month-old Apc^{Min} and $A33^{Dnmt3a}$;Apc^{Min} mice showing clustering of large polyps in $A33^{Dnmt3a}$;Apc^{Min} mice. Scale bar represents 1 cm.

of $A33^{Dnmt3a}$ and $A33^{wt}$ mice (Supplementary Figure 6*B*; data not shown), whereas expression of the Wnt-pathway target genes *Dkk-1*[31] and *Axin2/conductin*[32] was elevated in distal small intestines of $A33^{Dnmt3a}$ mice (Supplementary Figure 6*C*, *D*). In contrast, *Sfrp5* was strongly repressed in the distal small intestine of $A33^{Dnmt3a}$ mice, despite uniform rostrocaudal Dnmt3a transgene expression (Figure 5*A*). MSP analysis of DNA from normal mucosa and polyp tissues obtained from $A33^{Dnmt3a}$;Apc^{Min} mice also revealed hypermethylation of *Sfrp5* and to a lesser extent of *Sfrp1*, but not of *Sfrp2* (Figure 5*B–D*). We confirmed these observations by bisulfite sequencing of the *Sfrp5* promoter, and noted that *Sfrp5* was subject to incomplete promoter methylation (Figure 5*E*), consistent with frequent partial hypermethylation observed in many human tumor suppressor genes. Furthermore, the similar extent of methylation between normal mucosa and tumors of individual mice suggests that *Sfrp5* methylation precedes tumor formation.

Sfrp5 and Apc Cooperate in Suppressing Canonical Wnt Signaling

To assess how partial suppression of *Sfrp5* affects Wnt signaling under conditions of limiting Apc availability, we monitored canonical pathway activity in wild-type and Apc^{Min} MEFs, which lack *Sfrp5* expression. Exposure of Apc^{wt} MEFs to increasing concentrations of the Wnt3a resulted in dose-dependent activation of the *SuperTOPflash*-reporter (Figure 6*A*). Whereas analogous treatment of Apc^{Min} MEFs resulted in a shift to the "left" of the dose–response curve (Figure 6*B*), reporter activation in Apc^{Min} MEFs remained dependent on the presence of the Wnt ligand. This observation confirms that haplo-insufficiency for Apc suppresses its "gatekeeper" role in canonical Wnt-signaling.[33] Furthermore, transient expression of transfected *Sfrp5* showed that greater amounts of Sfrp5 were required to suppress TCF binding-mediated *SuperTOPflash* reporter activity in Apc^{Min} mice-derived MEFs than that obtained in Apc^{wt} MEFs. We infer from this experiment that partial suppression of *Sfrp5* expression (eg, in $A33^{Dnmt3a}$ mice), triggers a more profound canonical Wnt response in Apc^{Min} cells than in Apc^{wt} cells when exposed to identical concentrations of Wnt ligand. This observation is likely to translate to differential activation of various canonical-Wnt target genes in situ, because baseline expression of *Mmp7* and *CD44*, but not of *Cyclin D1* (Supplementary Figure 7), correlated inversely with *Sfrp5* expression level in the distal small intestine of $A33^{Dnmt3a}$;Apc^{Min} and Apc^{Min} mice.

Correlation Between DNMT3a, SFRP5, and AXIN2/CONDUCTIN Expression in Human CRCs

Paired human CRC specimens were analyzed to validate a causal relationship between aberrant *Dnmt3a* expression, suppression of *Sfrp5* and enhanced *Axin2/conductin* expression in $A33^{Dnmt3a}$;Apc^{wt} mice. We found tumor-specific overexpression of *DNMT3A* and *DNMT3B* in the same 4 of 9 samples; the remaining samples had comparable expression of these *DNMTs* between tumor and the paired healthy mucosa (Figure 7*A*, *B*). We also observed impaired *SFRP5* expression in 7 of 9 tumors, which coincided with the 4 tumors characterized by elevated *DNMT3a* expression (Figure 7*C*). In addition, 75% of samples in the latter tumor group (samples 2–4) were also characterized by elevated expression of *AXIN2/CONDUCTIN*, which is commonly coincides with hyperactivation of the canonical Wnt pathway (Figure 7*D*). Our results therefore provide evidence for a correlation between overexpression of de novo *DNMTs* and the expression levels of *SFRP5* and *AXIN2/CONDUCTIN*, which could be predicted and functionally rationalized using the corresponding mouse models of *Dnmt3a* (in this report) and *Dnmt3b*[29] overexpression.

Discussion

A correlation between cancer and aberrant methylation of genes with tumor suppressor activity is well documented, but it remains unclear whether increased de novo Dnmt activity can initiate tumorigenesis. Here we have shown that increasing Dnmt3a activity by a modest 4-fold in IECs is sufficient to trigger sporadic polyposis in

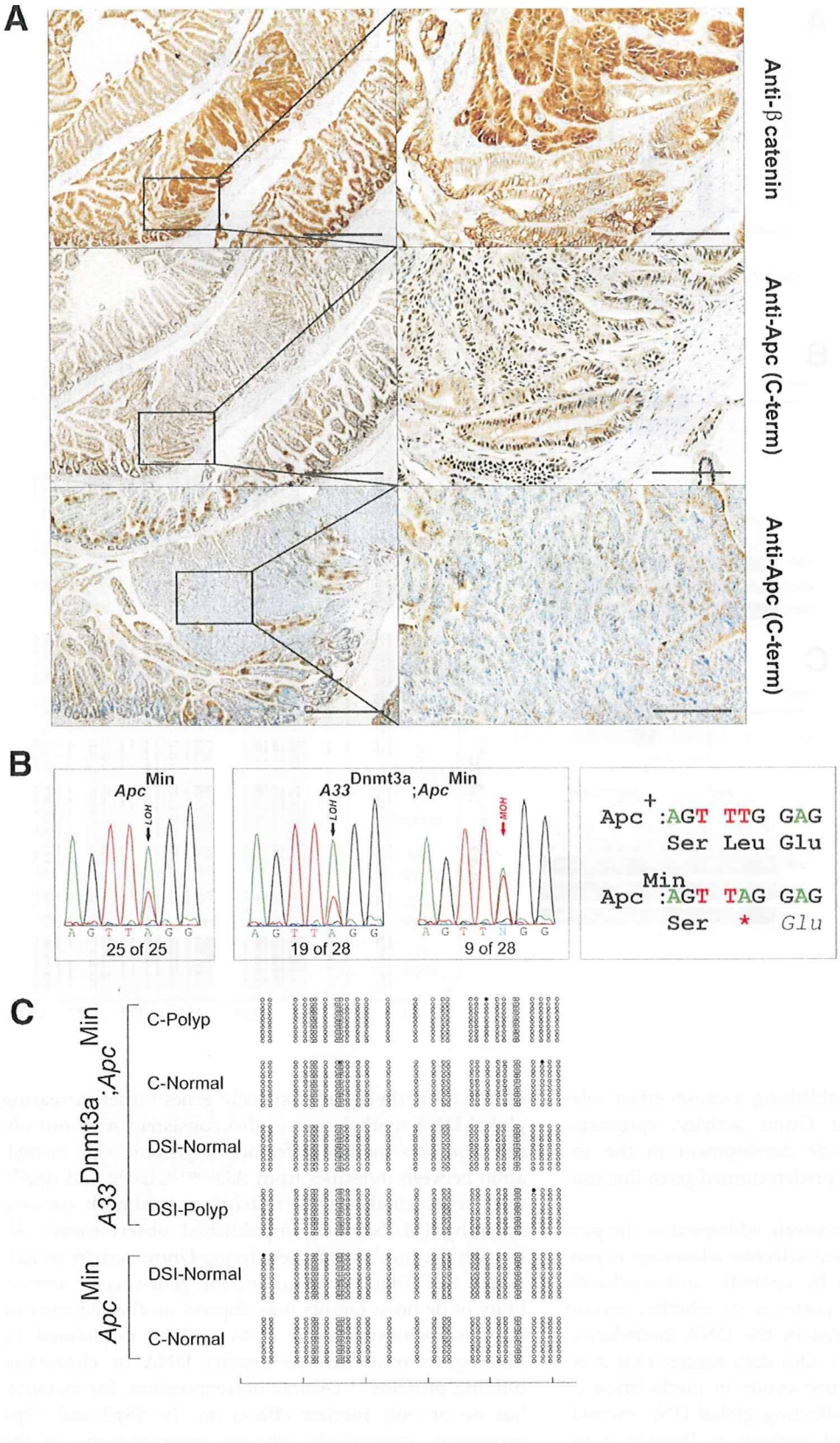

Figure 4. Intestinal polyposis in *A33*^{Dnmt3a};*Apc*^{Min} mice in the presence of full-length Apc. (*A*) Polyps and adjacent normal mucosa of distal small intestine (DSI) from *A33*^{Dnmt3a};*Apc*^{Min} mice were immunohistochemically stained for β-catenin or Apc and visualized at low (*left*; scale bar represents 500 μm) and higher magnification of boxed sections (*right*; scale bar represents 100 μm). Use of an antibody that recognizes the carboxyl-terminal portion of the full-length Apc detects polyps with either reduced (*middle*) or absent staining (*bottom*). (*B*) Representative, allele-specific nucleotide sequence of tumor DNA extracted from *Apc*^{Min} or *A33*^{Dnmt3a};*Apc*^{Min} mice and encoding the region around Leu_{580} of the Apc protein. (*C*) Bisulfite sequencing analysis of *Apc* in polyps and adjacent normal mucosa from DSI and colon (C) of *A33*^{Dnmt3a};*Apc*^{Min} mice. Horizontal lines represent individual sequences with open and full circles denoting unmethylated and methylated CpG residues, respectively. Each sequence block represents a single biological sample.

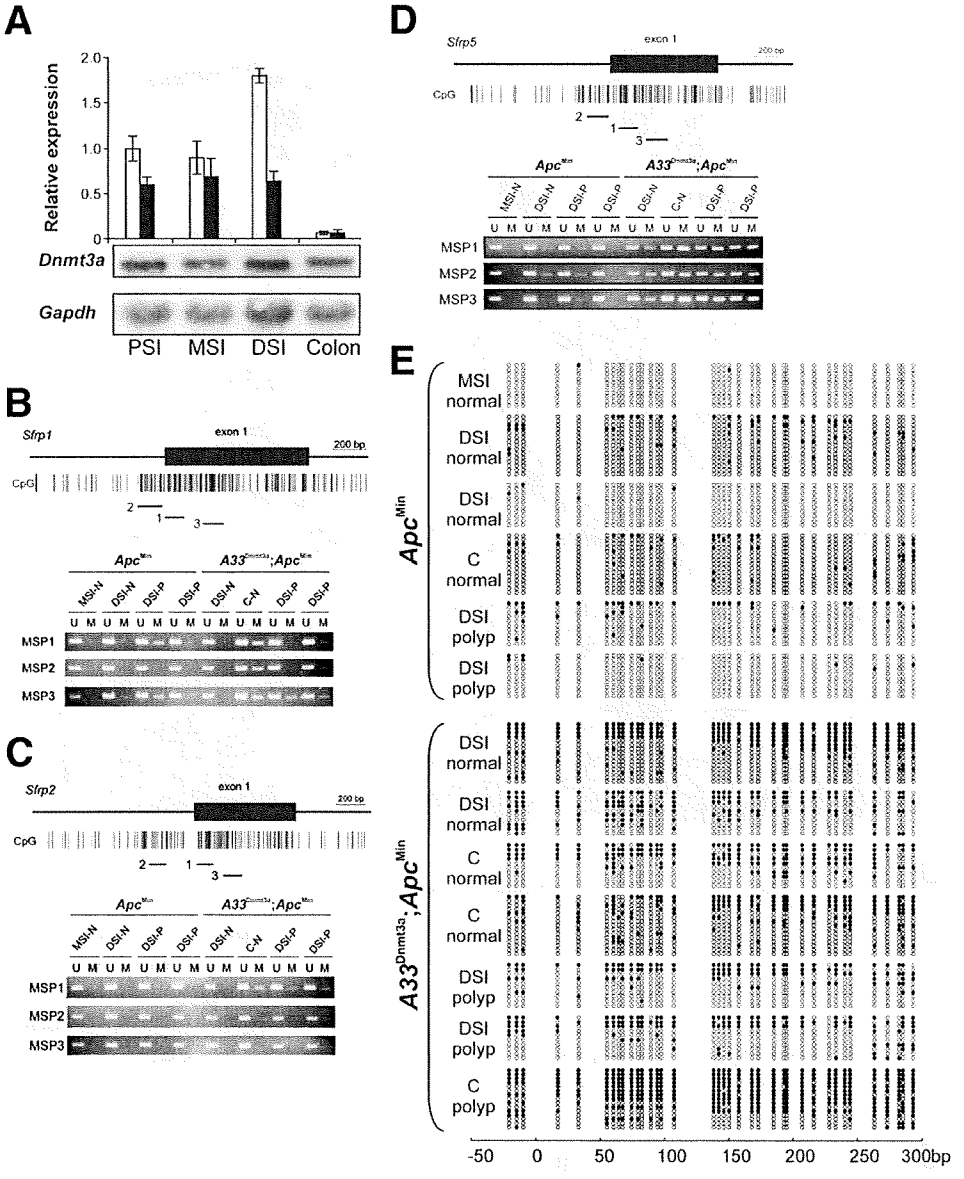

Figure 5. *Sfrp5* promoter hypermethylation in intestinal mucosa of $A33^{Dnmt3a}$ mice. (*A*) qPCR analysis of *Sfrp5* expression in IECs obtained from the indicated region of the intestinal tract of $A33^{Dnmt3a}$ (*solid bars*) and $A33^{wt}$ (*open bars*) mice. Data were normalized against *Gapdh* expression. Northern analysis of IECs obtained from $A33^{Dnmt3a}$ mice verifies uniform overexpression of the *Dnmt3a* transgene throughout the small intestine and colon. Mean ± SD; n = 3 (*B–D*) MSP analysis of promoter CpG islands of the *Sfrp1* (B), *Sfrp2* (C), and *Sfrp5* (D) genes in normal (N) and polyp (P) tissue. Numbers denote the regions amplified by PCR to yield the respective MSP1 to MSP3 amplicons. PCR amplification was carried out on bisulfite-treated genomic DNA isolated from individual polyp and normal mucosa of $A33^{Dnmt3a}$;Apc^{Min} and Apc^{Min} mice. (*E*) Bisulfite sequencing analysis of *Sfrp5* in polyps and adjacent normal mucosa from middle (MSI), distal small intestine (DSI), and colon (C) of $A33^{Dnmt3a}$;Apc^{Min} and Apc^{Min} mice. Horizontal lines represent individual sequences with open and full circles denoting unmethylated and methylated CpG residues, respectively. Each sequence block represents a single biological sample.

$A33^{Dnmt3a}$ mice, thereby establishing a cause-effect relationship between aberrant Dnmt activity, epigenetic modifications, and neoplastic development in the absence of any compounding, predetermined germ-line mutation.

A question not comprehensively addressed in the past is whether a tumor-associated selective advantage is provided to a subset of cells by sporadic and stochastic alterations in methylation patterns, or whether certain genes are specifically targeted by the DNA methylation machinery at high frequency. Our data suggest that overexpression of de novo Dnmts results in methylation of specific genes rather than affecting global DNA methylation, and is reminiscent of findings in *Dnmt3b* transgenic mice.[29] The conclusion that Dnmt overexpression results in methylation of specific genes rather increasing global DNA methylation is also consistent with our observation of a modest difference in genome-wide methylation between intestines from $A33^{Dnmt3a}$;Apc^{Min} and Apc^{Min} mice when analyzed by restriction landmark genome scanning (M. Samuel, unpublished observations). Although the mechanisms restricting Dnmt activity to particular CpG islands remain unclear, gene-specific accessibility of de novo Dnmts may depend on the sequence of non-heterochromatinized DNA and be modulated by binding to other (tissue-specific) DNA or chromatin binding proteins.[34] *Dnmt3a* overexpression, for instance, has no or only modest effects on the *Sfrp2* and *Sfrp1* promoters, respectively, whereas overexpression of the *Dnmt3b1* from the widely expressed *collagen 1A1* locus

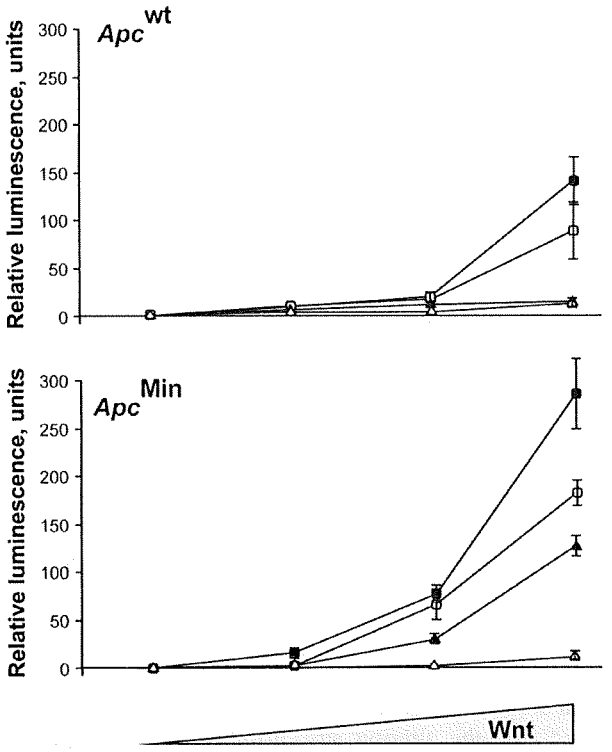

Figure 6. *Sfrp5* suppresses canonical Wnt-signaling less effectively in Apc^{Min} than in Apc^{wt} MEFs. Triplicate MEF cultures were transfected with *SuperTOPflash*-reporter plasmid together with increasing concentrations of the expression plasmid *pCMV-HA-SFRP5* (■ no plasmid; □ 20 ng/mL; ▲ 60 ng/mL; △ 200 ng/mL) and cultured for 48 hours in the presence of increasing concentrations of Wnt3a. Results were normalized against expression of Renilla luciferase. Note that MEFs do not express endogenous Sfrp5. Mean ± SD; $n = 3$.

yielded prominent, IEC-specific hypermethylation of *Sfrp2*, but not *Sfrp1*.[29] In contrast, *Apc* remained unmethylated in IECs of $Col1A1^{Dnmt3b}$ and $A33^{Dnmt3a}$ mice, while both Dnmt transgenes mediated extensive *Sfrp5* hypermethylation. Because *Col1A1* Dnmt3a mice exhibited neither aberrant *Sfrp2* and *Sfrp5* methylation nor developed polyps, differences between *Dnmt3a* overexpression levels conferred by the A33 and the *Col1A1* loci may help to specify the range of methylated target genes and thereby ultimately determine the extent of the (intestinal) phenotype in the 2 corresponding transgenic mouse strains. This notion is indirectly supported by our inability to derive live *A33* transgenic mice that overexpressed either *Dnmt1* or *Dnmt3b* (M. Samuel, unpublished observations), possibly resulting from transgene expression during transient activation of the *A33* locus in the preimplantation embryo[35] and embryonic lethality.

Methylation-associated gene silencing can act as a "second-hit" in genes linked to cancer initiation[36] and convergence of genetic mutations and epigenetic alterations in common cancer genes predicts a poor prognosis.[37] Indeed, partial rather than complete gene methylation seems to be the norm, and suggests a gene-dosage effect of the affected genes and pathways during tumorigenic processes. Because stringent regulation of Wnt signaling is important in self-renewing tissues and dysregulation

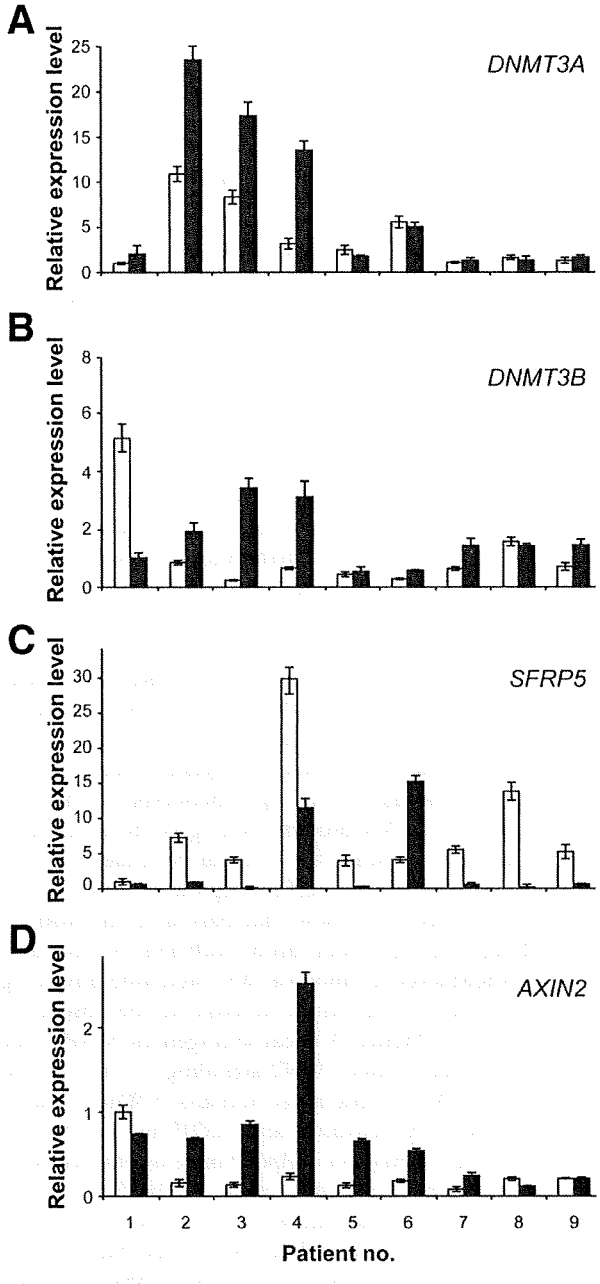

Figure 7. Correlation between *DNT3A*, *SFRP5* and *AXIN2* expression in paired colorectal cancer biopsies. TaqMan qPCR analysis of *DNMT3A* (*A*), *DNMT3B* (*B*), *SFRP5* (*C*), and *AXIN2/CONDUCTIN* (*D*) expression in tumors (*filled bars*) and normal distant mucosa (*open bars*). Results were normalized against *GAPDH* expression, and RNA was reverse transcribed on 2 separate occasions for TaqMan analysis in duplicate. Tumor samples comprised 2 cecal, 2 transverse, 2 sigmoid, and 3 rectal biopsies, and were obtained from 7 male and 2 female patients with a median age of 61 years (range, 47–78). Mean ± SD.

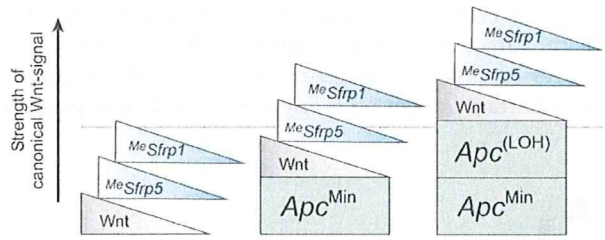

Figure 8. Model depicting the cumulative nature of (epi-)genetic events affecting Wnt signaling and polyposis in mice. Three separate situations schematically depict contributions to the canonical Wnt signaling pathway occuring in wild-type (wt), Apc^{Min} cells with 1 mutant *Apc* allele or in Apc^{Min} cells that have undergone LOH. The height of the boxes and triangles indicates additive signal strength attributed to an event with binary (genetic *Apc* mutation) or graded outcomes, such as the extent of available Wnt ligand (*grey*) or *Sfrp* gene methylation/silencing (*blue*). The dotted line indicates the threshold signal required for polyposis.

occurs in cancers, Apc^{Min} mice are a useful model to experimentally explore gene-dosage effects. In particular, phenotypically "silent" haploinsufficiency only becomes evident in Apc^{Min} mice after genetic or chemical challenge. Accordingly, reduced Dnmt1 activity promotes *Apc*-LOH and formation of microadenomas in Apc^{Min};*Dnmt1* hypomorphic compound mice. Furthermore, allele-specific expression ratios in CRC lesions of familial adenomatous polyposis patients reveal that small changes to expression of the remaining wild-type *APC* allele influences predisposition to tumorigenesis.[38] Meanwhile, SFRP and DKK-1 inhibit canonical WNT signaling, even in the presence of activating *CTNNB1* and *APC* mutations in humans[24,39] and in Apc^{Min} cells (Figure 6). Thus, (epi-)genetic mutations can simulate a haploinsufficient *Apc* phenotype in the presence of functional Apc protein, as long as the net effect of the mutations accounts for a signal equivalent to that associated with less than half the diploid *Apc* gene dosage (Figure 8). Indeed, we show that partial epimutation of several negative regulators can be sufficient to surmount the threshold level of canonical Wnt signaling physiologically tolerated by intestinal mucosa in the absence of Apc mutations (Figure 2). Because epigenetic *SFRP* silencing can further enhance WNT-signaling in the presence of biallelic *APC* mutations in humans,[24] Wnt signaling may not be fully activated after LOH in Apc^{Min} mice. Indeed, tumor formation in Apc^{Min} mice is retarded when compared with *Lgr5*-EGFP-creER T2;$Apc^{flox/flox}$ mice[40] where Cre-induced *Apc* inactivation results in an truncation that is more radical than in the Apc Min protein. Therefore, Dnmt3a-mediated silencing of *Sfrp5* (and to a lesser extent *Sfrp1*) may sensitize Wnt-target genes in $A33^{Dnmt3a}$;Apc^{Min} IECs before, and possibly after, LOH. Subsequent small and stochastic fluctuations in locally available Wnt ligand may (transiently) elevate canonical Wnt-signaling above the pathophysiologic threshold and provide the small proliferative advantage required for de novo tumorigenesis. Accordingly, differential expression of Sfrp5 (silenced by the $A33^{Dnmt3a}$ transgene) and Sfrp2 (silenced by the $Col1A1^{Dnmt3b}$ transgene) and/or differences in their binding specificity may explain why polyposis in $Col1A1^{Dnmt3b}$;Apc^{Min}, but not in $A33^{Dnmt3a}$;Apc^{Min} mice, remained strictly dependent on *Apc*-LOH.[29] Indeed, Sfrp5 is the most abundantly expressed Sfrp protein in epithelial cells of the intestinal crypt with a rostrocaudal expression gradient that peaks in the distal small intestine[41] and the largest accumulation of transcripts is found in positions of the putative stem cells.[42]

Dnmt overexpression occurs in various cancers of epithelial origin, including hypermethylator phenotype-positive gastric, colorectal, and breast cancers.[43] Furthermore, expression of *DNMT3A*, along with *DNMT3B* and *DNMT1* is progressively up-regulated in the colorectal adenoma–carcinoma sequence in humans,[44] and correlates with elevated *Dnmt3b* expression in polyps of Apc^{Min} mice.[8] Intriguingly, promoter methylation of *DNMT3L*, which encodes a catalytically inert protein that augments the activity of DNMT3A, is relaxed in some human cancers,[45] whereas reduced expression of miR-29 in lung cancer de-represses transcription of *DNMT3A* and *DNMT3B*.[46] In addition, recent evidence also suggests that some *Dnmt* genes may undergo cancer-specific splicing,[47] thereby altering susceptibility to transcriptional activity mediated by intron-specific binding of regulatory proteins.[48] Our observations support the use of DNA methyltransferase inhibitors for the therapeutic reversion of epigenetic mutations as a potential strategy for cancer therapy, and $A33^{Dnmt3a}$;Apc^{Min} mice may be helpful in exploring and assessing novel compounds designed to alleviate the toxicity of 5-azacytidine.[49] Such strategies could be used complementarily with attempts to dampen constitutive Wnt activation through the expression of signaling antagonists or molecules disrupting the transcriptionally active β-catenin/Tcf-1 complex.

Supplementary Data

Note: To access the supplementary material accompanying this article, visit the online version of *Gastroenterology* at www.gastrojournal.org, and at doi: 10.1053/j.gastro.2009.05.042.

References

1. Jones PA, Baylin SB. The fundamental role of epigenetic events in cancer. Nat Rev Genet 2002;3:415–428.
2. Jones PA, Laird PW. Cancer epigenetics comes of age. Nat Genet 1999;21:163–167.
3. el-Deiry WS, Nelkin BD, Celano P, et al. High expression of the DNA methyltransferase gene characterizes human neoplastic cells and progression stages of colon cancer. Proc Natl Acad Sci U S A 1991;88:3470–3474.
4. Feinberg AP, Vogelstein B. Hypomethylation distinguishes genes of some human cancers from their normal counterparts. Nature 1983;301:89–92.
5. Issa JP. CpG-island methylation in aging and cancer. Curr Top Microbiol Immunol 2000;249:101–118.

6. Baylin SB, Hoppener JW, de Bustros A, et al. DNA methylation patterns of the calcitonin gene in human lung cancers and lymphomas. Cancer Res 1986;46:2917–2922.
7. Herman JG, Baylin SB. Gene silencing in cancer in association with promoter hypermethylation. N Engl J Med 2003;349:2042–2054.
8. Lin H, Yamada Y, Nguyen S, et al. Suppression of intestinal neoplasia by deletion of Dnmt3b. Mol Cell Biol 2006;26:2976–2983.
9. Wu J, Issa JP, Herman J, et al. Expression of an exogenous eukaryotic DNA methyltransferase gene induces transformation of NIH 3T3 cells. Proc Natl Acad Sci U S A 1993;90:8891–8895.
10. Chan AO, Rashid A. CpG island methylation in precursors of gastrointestinal malignancies. Curr Mol Med 2006;6:401–408.
11. Suzuki H, Gabrielson E, Chen W, et al. A genomic screen for genes upregulated by demethylation and histone deacetylase inhibition in human colorectal cancer. Nat Genet 2002;31:141–149.
12. Schmidt WM, Sedivy R, Forstner B, et al. Progressive up-regulation of genes encoding DNA methyltransferases in the colorectal adenoma-carcinoma sequence. Mol Carcinog 2007;46:766–772.
13. Bestor TH. Unanswered questions about the role of promoter methylation in carcinogenesis. Ann N Y Acad Sci 2003;983:22–27.
14. Fearon ER, Vogelstein B. A genetic model for colorectal tumorigenesis. Cell 1990;61:759–767.
15. Sancho E, Batlle E, Clevers H. Signaling pathways in intestinal development and cancer. Annu Rev Cell Dev Biol 2004;20:695–723.
16. Kinzler KW, Vogelstein B. Lessons from hereditary colorectal cancer. Cell 1996;87:159–170.
17. Kawano Y, Kypta R. Secreted antagonists of the Wnt signalling pathway. J Cell Sci 2003;116:2627–2634.
18. Ward RL, Turner J, Williams R, et al. Routine testing for mismatch repair deficiency in sporadic colorectal cancer is justified. J Pathol 2005;207:377–384.
19. Frommer M, McDonald LE, Millar DS, et al. A genomic sequencing protocol that yields a positive display of 5-methylcytosine residues in individual DNA strands. Proc Natl Acad Sci U S A 1992;89:1827–1831.
20. Johnstone CN, Tebbutt NC, Abud HE, et al. Characterization of mouse A33 antigen, a definitive marker for basolateral surfaces of intestinal epithelial cells. Am J Physiol GastrointestLiver Physiol 2000;279:G500–G510.
21. Lakso M, Pichel JG, Gorman JR, et al. Efficient in vivo manipulation of mouse genomic sequences at the zygote stage. Proc Natl Acad Sci U S A 1996;93:5860–5865.
22. Welt S, Divgi CR, Real FX, et al. Quantitative analysis of antibody localization in human metastatic colon cancer: a phase I study of monoclonal antibody A33. J Clin Oncol 1990;8:1894–1906.
23. Esteller M, Sparks A, Toyota M, et al. Analysis of adenomatous polyposis coli promoter hypermethylation in human cancer. Cancer Res 2000;60:4366–4371.
24. Suzuki H, Watkins DN, Jair KW, et al. Epigenetic inactivation of SFRP genes allows constitutive WNT signaling in colorectal cancer. Nat Genet 2004;36:417–422.
25. Nathke IS, Adams CL, Polakis P, et al. The adenomatous polyposis coli tumor suppressor protein localizes to plasma membrane sites involved in active cell migration. J Cell Biol 1996;134:165–179.
26. Sansom OJ, Meniel VS, et al. Myc deletion rescues Apc deficiency in the small intestine. Nature 2007;446:676–679.
27. Turker MS. Gene silencing in mammalian cells and the spread of DNA methylation. Oncogene 2002;21:5388–5393.
28. Menschikowski M, Hagelgans A, Gussakovsky E, et al. Differential expression of secretory phospholipases A2 in normal and malignant prostate cell lines: regulation by cytokines, cell signaling pathways, and epigenetic mechanisms. Neoplasia 2008;10:279–286.
29. Linhart HG, Lin H, Yamada Y, et al. Dnmt3b promotes tumorigenesis in vivo by gene-specific de novo methylation and transcriptional silencing. Genes Dev 2007;21:3110–3122.
30. Kane MF, Loda M, Gaida GM, et al. Methylation of the hMLH1 promoter correlates with lack of expression of hMLH1 in sporadic colon tumors and mismatch repair-defective human tumor cell lines. Cancer Res 1997;57:808–811.
31. Niida A, Hiroko T, Kasai M, et al. DKK1, a negative regulator of Wnt signaling, is a target of the β-catenin/TCF pathway. Oncogene 2004;23:8520–8526.
32. Jho E, Zhang T, Domon C, et al. Wnt/β-catenin/TcF signaling induces the transcription of axin-2, a negative regulator of the signaling pathway. Mol Cell Biol 2002;22:1172–1183.
33. Li Q, Ishikawa TO, Oshima M, et al. The threshold level of adenomatous polyposis coli protein for mouse intestinal tumorigenesis. Cancer Res 2005;65:8622–8627.
34. Fuks F, Burgers WA, Godin N, et al. Dnmt3a binds deacetylases and is recruited by a sequence-specific repressor to silence transcription. EMBO J 2001;20:2536–2544.
35. Abud HE, Johnstone CN, Tebbutt NC, et al. The murine A33 antigen is expressed at two distinct sites during development, the ICM of the blastocyst and the intestinal epithelium. Mech Dev 2000;98:111–114.
36. Costello JF, Plass C. Methylation matters. J Med Genet 2001;38:285–303.
37. Chan TA, Glockner S, Yi JM, et al. Convergence of mutation and epigenetic alterations identifies common genes in cancer that predict for poor prognosis. PLoS Med 2008;5:e114.
38. Yan H, Dobbie Z, Gruber SB, et al. Small changes in expression affect predisposition to tumorigenesis. Nat Genet 2002;30:25–26.
39. Aguilera O, Fraga MF, Ballestar E, et al. Epigenetic inactivation of the Wnt antagonist DICKKOPF-1 (DKK-1) gene in human colorectal cancer. Oncogene 2006;25:4116–4121.
40. Barker N, Ridgway RA, et al. Crypt stem cells as the cells-of-origin of intestinal cancer. Nature 2009;457:608–611.
41. Sabates-Bellver J, Van der Flier LG, de Palo M, et al. Transcriptome profile of human colorectal adenomas. Mol Cancer Res 2007;5:1263–1275.
42. Gregorieff A, Pinto D, Begthel H, et al. Expression pattern of Wnt signaling components in the adult intestine. Gastroenterology 2005;129:626–638.
43. Kanai Y, Hirohashi S. Alterations of DNA methylation associated with abnormalities of DNA methyltransferases in human cancers during transition from a precancerous to a malignant state. Carcinogenesis 2007;28:2434–2442.
44. Schmidt WM, Sedivy R, Forstner B, et al. Progressive up-regulation of genes encoding DNA methyltransferases in the colorectal adenoma-carcinoma sequence. Mol Carcinog 2007;46:766–772.
45. Gokul G, Gautami B, Malathi S, et al. DNA methylation profile at the DNMT3L promoter: a potential biomarker for cervical cancer. Epigenetics 2007;2:80–85.
46. Fabbri M, Garzon R, Cimmino A, et al. MicroRNA-29 family reverts aberrant methylation in lung cancer by targeting DNA methyltransferases 3A and 3B. Proc Natl Acad Sci U S A 2007;104:15805–15810.
47. Ostler KR, Davis EM, Payne SL, et al. Cancer cells express aberrant DNMT3B transcripts encoding truncated proteins. Oncogene 2007;26:5553–5563.
48. Gowher H, Stuhlmann H, Felsenfeld G. Vezf1 regulates genomic DNA methylation through its effects on expression of

DNA methyltransferase Dnmt3b. Genes Dev 2008;22:2075–2084.
49. Stresemann C, Brueckner B, Musch T, et al. Functional diversity of DNA methyltransferase inhibitors in human cancer cell lines. Cancer Res 2006;66:2794–2800.

Received October 19, 2008. Accepted May 14, 2009.

Reprint requests

Address requests for reprints to: Matthias Ernst, Ludwig Institute for Cancer Research, Post Office Box 2008 Royal Melbourne Hospital, VIC 3050, Australia. e-mail: Matthias.Ernst@ludwig.edu.au.

Acknowledgments

Michael S. Samuel is currently at The Beatson Institute for Cancer Research, Garscube Estate, Switchback Road, Bearsden, Glasgow G61 1BD, United Kingdom. Paul M. Waring is currently at the School of Pathology and Laboratory Medicine, The University of Western Australia, Crawley WA 6009, Australia.

The authors thank Dianne Grail, Valerie Feakes and the members of Ludwig Institute's Animal Facility for excellent technical assistance.

Conflict of interest

The authors disclose no conflicts.

Funding

M.S. and P.M.W. were supported by a Grant-in-Aid from the Cancer Council Victoria. M.E. and J.K.H. were supported by the National Health and Medical Research Council of Australia (NHMRC) and by NHMRC Senior Research Fellowships. RW is supported by the NSW Cancer Council and the NHMRC.

Supplementary Methods

Generation of A33^{Dnmt3a} Mice

To generate the *pA33*$^{LneoL\text{-}Dnmt3a}$ targeting vector, a Dnmt3a1-encoding cDNA, was used to substitute the ΔN131-βcat coding sequence in the *pA33*$^{LneoL\text{-}\Delta N131\text{-}\beta cat}$ plasmid.[1] Inclusion of an LSL cassette comprising a second internal ribosome entry site IRES fused to the neomycin (*neo*) resistance gene, takes advantage of transient *gpA33* activity in the inner cell mass and corresponding embryonic stem (ES) cells at the blastocyst stage.[2] Excision of the LSL cassette confers transgene expression to all IECs, including those of the epithelial stem cell compartment of the small intestine and colon as assessed by lineage trace experiments in analogously constructed *A33* CrePR2 mice[3] (Ernst, unpublished data). We electroporated 129/SvJ ES cells with linearized *pA33*$^{LneoL\text{-}Dnmt3a}$ vector and genotyped G418-resistant clones by Southern blotting, which yielded a targeting efficiency of 24%. Three independently derived *A33*$^{LSL\text{-}Dnmt3a}$ ES cell lines were injected into C57Bl/6 blastocysts and Cre-mediated excision of the LSL cassette in the germline occurred after the mating of chimeric males with female C57Bl/6 E2a: Cre mice.[4] Resulting *A33*$^{LSL\text{-}Dnmt3a}$ and *A33*^{Dnmt3a} progeny were identified by Southern blotting, bred to homozygosity, and back-crossed for 8 generations to the C57Bl/6 background. We monitored distribution of different *gpA33* alleles by PCR genotyping of tail biopsy DNA using primers (Supplementary Table 1) that yielded amplicons of ~420 bp (*A33*$^{LSL\text{-}Dnmt3a}$) and ~370 bp (*A33*^{Dnmt3a}), respectively. All mice were housed in open-top cages.

Histology, Immunocytochemistry, and Immunohistochemistry

To retrieve antigens, rehydrated sections were boiled in 1 mmol/l EDTA pH 8.0 (anti-β-catenin), 0.01 mol/l sodium citrate pH 6.0 (anti-Apc), or 0.1 mol/l Tris-HCl pH 9.0 (anti-Dnmt3a) and incubated with primary antibody diluted in phosphate-buffered saline (PBS) or CAS-Block (Invitrogen, Carlsbad, CA) at room temperature for 1 hour followed by HRP-conjugated secondary antibody for 30 minutes. Diaminobenzidine (Dako, Carpentaria, CA) was used for visualization and sections were counterstained with hematoxylin. Antibody dilutions were as follows: mouse anti-bromodeoxyuridine (1:100; Dako), rabbit anti-mA33 antigen (1:100; Johnstone et al[5]), mouse anti-β-catenin (1:100; BD Biosciences, Bedford, MA), rabbit anti-Apc antibody (1:100; Nathke et al),[6] rabbit anti-hDnmt3a (1:100; Calbiochem, San Diego, CA), anti-mouse HRP (1:200; Bio-Rad, Hercules, CA) and anti-rabbit HRP (1:200; Bio-Rad).

mRNA Expression Analysis

To release IECs from stroma, small intestines and colons were incubated in PBS containing 3 mmol/L EDTA and 0.5 mmol/L DTT, followed by total RNA extraction using TRIzol (Invitrogen). qPCR expression analysis was carried out on oligo dT- or random-primed cDNA prepared by Superscript III reverse transcriptase (Invitrogen) with the indicated primers (Supplementary Table 1) and quantified by the SYBR-Green dye (Fisher Biotech, Wembley, Western Australia) method using the Rotorgene RG-3000 system (Qiagen, Doncaster VIC, Australia). Taqman analysis (Applied Biosystems) was performed on an AB7300 system (Applied Biosystems). Data were expressed in units relative to GAPDH or 18s RNA expression level.

Cell Culture and Transfections

MEFs were derived from E13 embryos and propagated in DMEM supplemented with 15% fetal bovine serum. Wnt3a-conditioned medium was a gift from Dr Liz Vincan (Peter MacCallum Cancer Institute, Melbourne, Australia) and Ms Nicole Church (JPSL, Ludwig Institute for Cancer Research, Melbourne, Australia). MEFs were plated onto 6-well plates at 5×10^4 cells per well in DMEM and replaced with Wnt3a-containing DMEM. Transfections were carried out using FuGENE 6 transfection reagent (Roche, Basel, Switzerland), 200 ng *pSuperTOPflash*,[7] 4 ng pRL-CMV and the indicated amount of pCMV-HA-SFRP5 expression construct. Two days later, cultures were processed using the Dual-Luciferase Reporter Assay kit (Promega, Madison, WI) and luminescence was measured using a Lumistar Galaxy luminometer (Dynatech Laboratories, Orlando, FL).

Methylation Analysis

Bisulfite treatment of genomic DNA was carried out as described[8] and MSP (primers in Supplemnetal Table 2) was performed in 25 μl containing 67 mmol/l Tris-HCl (pH 8.8), 16.6 mmol/l $(NH_4)_2SO_4$, 6.7 mmol/l $MgCl_2$, 10 mmol/l 2-mercaptoethanol, 1.25 mmol/l dNTP, 0.4 μmol/l per primer, and 0.5 U of JumpStart REDTaq DNA Polymerase (Sigma, St Louis, MO) for 35 cycles (95°C for 30 seconds; 60°C for 30 seconds; 72°C for 30 seconds). For bisulfite sequencing, PCR amplicons (35 cycles; 95°C for 60 seconds; 60°C for 60 seconds; 72°C for 60 seconds) were cloned into pCR2.1 TOPO and sequenced using the ABI3100 system (Applied Biosystems).

References

1. Orner GA, Dashwood WM, Blum CA, et al. Response of Apc(min) and A33 (delta N beta-cat) mutant mice to treatment with tea, sulindac, and 2-amino-1-methyl-6-phenylimidazo[4,5-b]pyridine (PhIP). Mutat Res 2002;506–507:121–127.
2. Abud HE, Johnstone CN, Tebbutt NC, et al. The murine A33 antigen is expressed at two distinct sites during development, the ICM of the blastocyst and the intestinal epithelium. Mech Dev 2000;98: 111–114.
3. Malaterre J, Carpinelli M, Ernst M, et al. c-Myb is required for progenitor cell homeostasis in colonic crypts. Proc Natl Acad Sci U S A 2007;104:3829–3834.

4. Lakso M, Pichel JG, Gorman JR, et al. Efficient in vivo manipulation of mouse genomic sequences at the zygote stage. Proc Natl Acad Sci U S A 1996;93:5860–5865.
5. Johnstone CN, Tebbutt NC, Abud HE, et al. Characterization of mouse A33 antigen, a definitive marker for basolateral surfaces of intestinal epithelial cells. Am J Physiol Gastrointest Liver Physiol 2000;279:G500–G510.
6. Nathke IS, Adams CL, Polakis P, et al. The adenomatous polyposis coli tumor suppressor protein localizes to plasma membrane sites involved in active cell migration. J Cell Biol 1996; 134:165–179.
7. Veeman MT, Slusarski DC, Kaykas A, et al. Zebrafish prickle, a modulator of noncanonical Wnt/Fz signaling, regulates gastrulation movements. Curr Biol 2003;13:680–685.
8. Frommer M, McDonald LE, Millar DS, et al. A genomic sequencing protocol that yields a positive display of 5-methylcytosine residues in individual DNA strands. Proc Natl Acad Sci U S A 1992; 89:1827–1831.

Supplementary Table 1. Nucleotide Sequence for Primers Used for Genotyping and Quantitative RT-PCR

Gene	Sense primer	Antisense primer
Apc (ex16)	5′-TCACCGGAGTAAGCAGAGACAC	5′-TTTGGCATAAGGCATAGAGCAT
Dnmt3a	5′-CTCCATAAAGCAGGGCAAAG	5′-AGTCTCTGCCTCGCCAAG
Dnmt3b	5′-GAATGCGCTGGGTACAGT	5′-GCCACCAGTTTGTCAGCA
Gapdh	5′-CAACTCACTCAAGATTGTCAGCAA	5′-TACTTGGCAGGTTTCTCCAGGC
genotype (*IRES-neo*)	5′-AATGGCTCTCCTCAA	5′-CAATAGCAGCCAGTC
genotype (*IRES-Dnmt3a*)	5′-AATGGCTCTCCTCAA	5′-GTGTCACTGCTTTCC
Mlh1	5′-AGGAGTCGACCCTCTCAGG	5′-CCATACACTTCGCCTTGGAT
Gsk3b	5′-CCGTCTGCTGGAGTACACAC	5′-AGCATGTGGAGGGATAAGGA
Dkk1	5′-CTGAAGATGAGGAGTGCGGCTC	5′-GGCTGTGGTCAGAGGGCATG
Axin2	5′-CCAACACTTTGGCACAGCTA	5′-TGCCAGTTTCTTTGGCTCTT
Mmp7	5′-GAGATGTGAGCGCACATCAGTG	5′-GATGTAGGGGGAGAGTTTTCCAGT
Cd44	5′-GTCTGCATCGCGGTCAATAG	5′-GGTCTCTGATGGTTCCTTGTTC
Ccnd1	5′-GCACAACGCACTTTCTTTCCA	5′-CGCAGGCTTGACTCCAGAAG
Sfrp5	5′-AACAGATGTGCTCCAGTGACTTT	5′-GGGATAGGAGAACATGAATTTGAC
*SFRP5**	taqman probe Hs00602456_m1	
*DNMT3A**	taqman probe Hs00169366_m	
*AXIN2**	taqman probe Hs00610344_m1	
*GAPDH**	taqman probe Hs99999905_m1	

All genes are mouse, except those denoted by *, which are human genes.

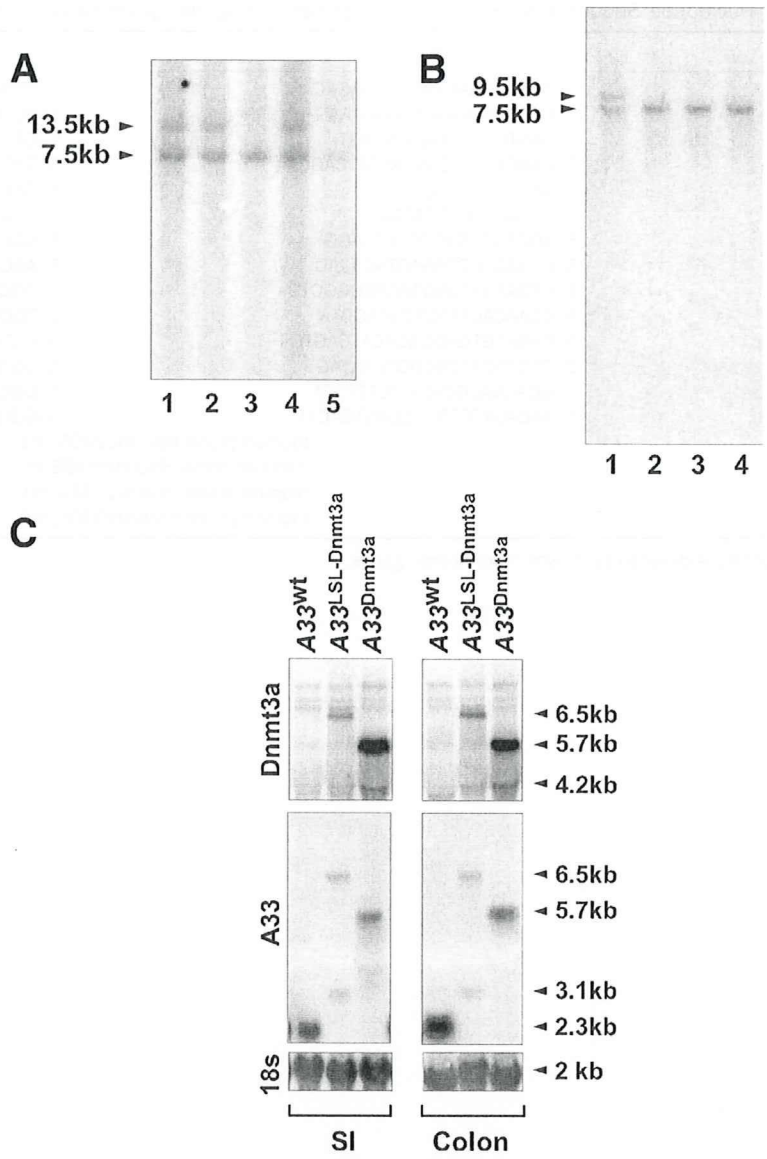

Supplementary Figure 1. Genetic characterization of $A33^{Dnmt3a}$ mice. (*A*) Southern Blot analysis of *A33* targeted ES cells. DNA prepared from G418-resistant ES cell clones was digested with *Eco*RV and subjected to Southern analysis using an [α-^{32}P]ATP-labeled (3,000 Ci/mmol/L; GE Biosciences, Rydalmere NSW, Australia) probe denoted by (*) in Figure 1*A*. Lanes 1, 2, and 4 correspond to clones which had undergone homologous recombination. The 7.5-kb band corresponds to the wild-type allele and the 13.5-kb band corresponds to the targeted $A33^{LSL\text{-}Dnmt3a}$ allele. (*B*) Southern Blot analysis genomic DNA of a representative litter following Cre-mediated recombination in vivo. Male $A33^{LSL\text{-}Dnm3a/+}$ mice were mated with female E2a:Cre transgenic mice and tail biopsy DNA was digested with *Eco*RV and subjected to Southern analysis as described. Lane 2 contains genomic DNA from a resulting $A33^{Dnm3a/+}$ mouse and the 9.5-kb band corresponds to the targeted $A33^{Dnm3a}$ allele. (*C*) Northern Blot analysis for *Dnmt3a* and *A33* antigen expression in *A33* knock-in mutant mice. Total cytoplasmic RNA (25 μg), prepared from IECs of mice homozygous for the indicated genotype were electrophoresed, blotted on duplicate Genescreen Plus nylon membranes (Perkin Elmer, Boston, MA) and hybridized with [α-^{32}P]ATP-labeled (3,000 Ci/mmol/L; GE Biosciences) partial cDNAs corresponding to *gpA33* and *Dnmt3a*, respectively. A probe against 18S rRNA (5′-CGGCA TGTAT TAGCT CTAGA ATTAC CACAG-3′) was used to assess RNA loading. Wild-type ($A33^{Wt}$) mice show weak endogenous *Dnmt3a* (4.2 kb) and prominent *gpA33* expression (2.3 kb). $A33^{LSL\text{-}Dnmt3a}$ mice express a 6.5kb *A33-neo-Dnmt3a* mRNA species alongside a weaker 3.1-kb *A33-neo* mRNA species, whereas analysis of $A33^{Dnmt3a}$ mice reveals a 5.7-kb transcript corresponding to bicistronic *A33-Dnmt3a* mRNA.

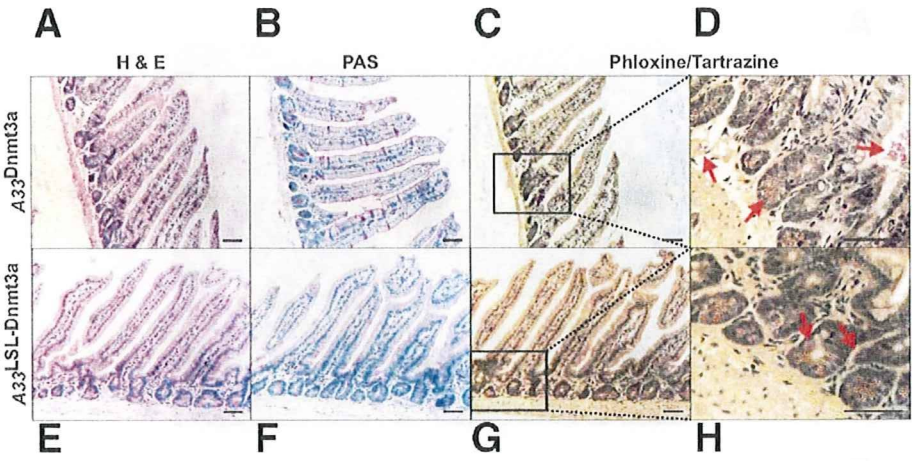

Supplementary Figure 2. Epithelial homeostasis is unaffected in *A33*^{Dnmt3a} "knock-in" mutant mice. Tissue sections from small intestines of *A33*^{Dnmt3a} (*A–D*) and *A33*$^{LSL\text{-}Dnmt3a}$ (*E–H*) mice were stained with hematoxylin and eosin (*A*, *E*). Staining for periodic acid-Schiff (*B*, *F*) was carried out according to manufacturer's instructions (Sigma) by treating dehydrated sections briefly in 1% periodic acid solution before incubating in Schiff's reagent for 20 minutes and 1% sodium metabisulfite for 5 minutes to visualize Goblet cells. Paneth cells (*red arrows*) were visualized by phloxine and tartrazine stains (*C* and *G* and respective enlargements of boxed sections in *D* and *H*) of deparaffinized and hydrated sections in alum hematoxylin solution (Sigma) for 5 minutes, rinsing and incubating in 0.5% phloxine (Sigma) in 0.5% aqueous calcium chloride for 20 minutes. After rinsing in tap water, sections were left in a saturated solution of tartrazine (Sigma) in 2-ethoxy ethanol, until all color was leached from the section except for the Paneth cells, which remained red. Sections were washed in 95% ethanol, dehydrated, and mounted in DPX. All scale bars represent 50 μm.

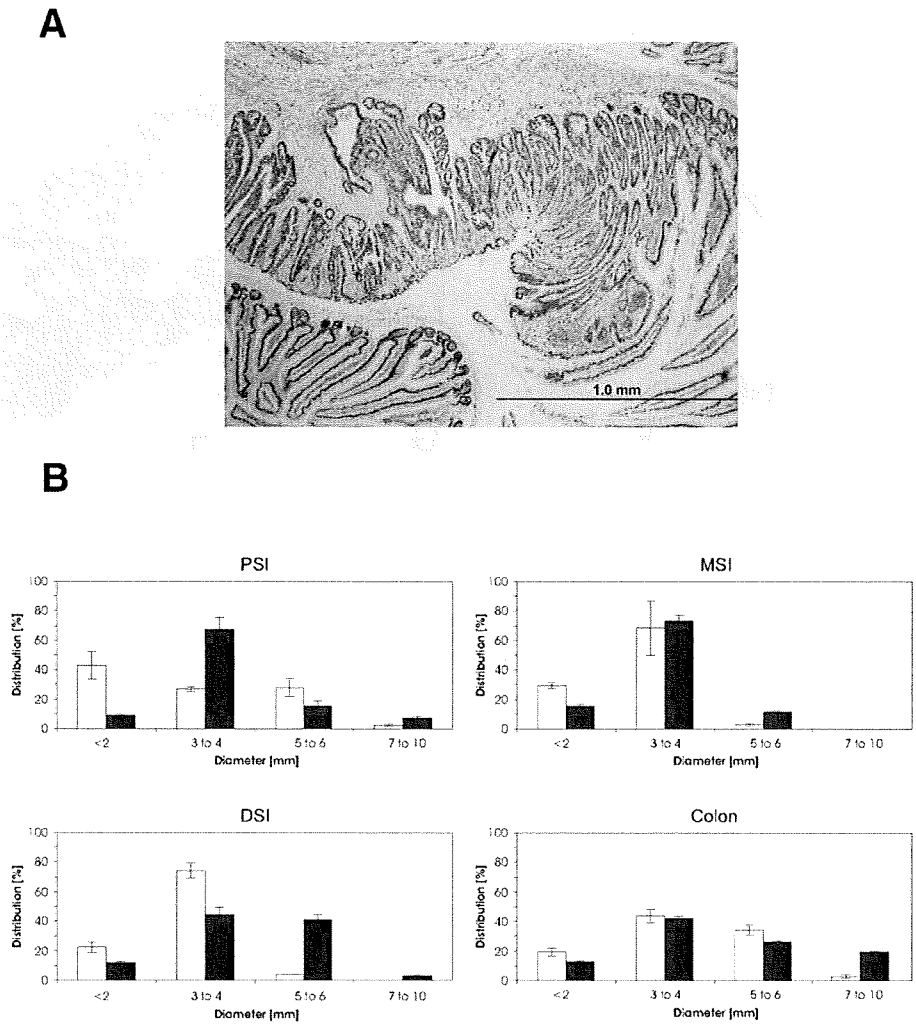

Supplementary Figure 3. Polyp size distribution in transgene positive lesions in *A33*^{Dnmt3a} mice. (*A*) Dnmt3a-specific immunohistochemical staining of a colonic polyp from a *A33*^{Dnmt3a} mouse. The scale bar represents 1 mm. (*B*) Size distribution of intestinal polyps in the proximal (PSI), middle (MSI), and distal small intestine (DSI) as well as colon of *Apc*^{Min} (open bars; $n = 28$) and *A33*^{Dnmt3a};*Apc*^{Min} mice (filled bars; $n = 18$).